

## Structure and Mechanical Properties of Crosslinked Glycidyl Azide Polymers via Click Chemistry as Potential Binder of Solid Propellant

Chong Hu,<sup>1</sup> Xiang Guo,<sup>2</sup> Yihan Jing,<sup>3</sup> Jun Chen,<sup>1</sup> Chao Zhang,<sup>3</sup> Jin Huang<sup>1</sup>

<sup>1</sup>College of Chemical Engineering, Wuhan University of Technology, Wuhan 430070, China

<sup>2</sup>The 42nd Institute of the Fourth Academy of China Aerospace Science and Technology Corporation (CASC), Xiangyang 441003, China

<sup>3</sup>School of Engineering, Sun Yat-Sen University, Guangzhou 510275, China

C.H. and X.G. contributed equally to this work.

Correspondence to: J. Huang (E-mail: huangjin@iccas.ac.cn)

**ABSTRACT:** Depending upon the advantages of high efficiency, insensitivity to humidity and so on, the reaction of azide groups in glycidyl azide polymers (GAP) with alkynyl compounds has been used as a substitute of the urethane curing strategy to develop GAP-based binder for solid propellant. In this work, an alkynyl compound of dimethyl 2,2-di(prop-2-ynyl)malonate (DDPM) reacted with GAP to produce new crosslinked materials under the catalysis of Cu(I)Cl at ambient temperature, and showed great potential as a binder in composite propellant. As the feeding molar ratio of DDPM vs. GAP increased from 1 : 1 to 5 : 1, the crosslinking densities of as-prepared materials gradually increased, together with simultaneous enhancement of Young's modulus and tensile strength. The breaking elongation showed the maximum value of ca. 82% when the feeding molar ratio of DDPM vs. GAP was 3 : 1. In addition, with an increase of the crosslinking densities, the glass transition temperatures of as-prepared materials significantly increased from  $-43.9^{\circ}\text{C}$  to  $-5.1^{\circ}\text{C}$  while the mechanical loss peaks also gradually broadened and shifted up to high temperature, and even presented two peaks at the feeding molar ratio of DDPM vs. GAP higher than 4 : 1. It indicated that the formation of triazole-based network resulted in structural heterogeneity in the as-prepared materials. © 2014 Wiley Periodicals, Inc. *J. Appl. Polym. Sci.* **2014**, *131*, 40636.

**KEYWORDS:** crosslinking; mechanical properties; structure; property relations

Received 5 January 2014; accepted 24 February 2014

DOI: 10.1002/app.40636

### INTRODUCTION

Glycidyl azide polymer (GAP) is widely accepted as a binder in a composite solid rocket propellants by virtue of high density, great formation enthalpy and low glass-transition temperature.<sup>1,2</sup> Although the highly polarity of azide groups and poor flexibility of backbone usually resulted in inferior mechanical behaviors of GAP,<sup>3</sup> hydroxyl-terminated GAP is still used to develop high performance energetic materials via the reaction with multifunction isocyanates.<sup>4</sup> Such urethane curing strategy can contribute to good mechanical properties and better resistance to aging for propellant.<sup>5</sup> Furthermore, many factors<sup>6,7</sup> including the type of multifunction isocyanates, the molar ratio of NCO/OH, the curing condition (especially for curing temperature) and so on, can be taken into consideration to regulate microstructure and mechanical properties of as-prepared GAP-based materials for meeting the requirements of composite solid propellant.<sup>8</sup> Various diisocyanates, such as toluene diisocyanate (TDI), isophorone diisocyanate (IPDI), and methylene dicyclohexyl isocyanate

(MDCI), have been used as the curing agents of hydroxyl-terminated GAP respectively, and showed significant impact on mechanical properties of as-prepared materials.<sup>9</sup> Higher reactivity of aromatic diisocyanate was easy to induce side reactions of forming biuret and allophanate linkages, and thus resulted in poorer mechanical properties in contrast to the GAP-based materials cured with aliphatic diisocyanate.<sup>9</sup> For the network-structured materials, crosslinking density is a key structural parameter to determine mechanical performances. In such urethane curing system, the molar ratio of NCO/OH is suitable to regulate the crosslinking density of the as-prepared materials by changing the feeding ratio of polyols and multifunctional isocyanates.<sup>10</sup> Usually, an increase in the molar ratio of NCO/OH can enhance crosslinking density, and hence simultaneously, lead to the increase of tensile strength and modulus with an expense of elongation. In addition, moderate and stable kinetics process is required for the preparation of composite solid propellant. As a result, the curing temperature, an important factor to curing

kinetics process, must be matched with the type of curing agents. When the GAP were cured with different diisocyanates at 30°C,<sup>11</sup> both GAP/TDI and GAP/IPDI systems obviously showed a two-stage reaction due to the difference in the reactivity of two isocyanate groups in the same curing agent, resulting in the instability of curing kinetics process. Although increasing curing temperature can make such two-stage reaction narrow down and even vanish, too fast and severe curing kinetics process under higher temperature usually leads to the decrease in the quality of composite solid propellant.

Despite that the urethane curing strategy has been widely applied in the field of composite solid propellant, there are still many shortcomings including high toxicity of diisocyanate, humidity-sensitivity of curing process, harsh curing, and storage conditions, generation of nitroso derivatives due to side reaction between urethane and nitrate-ester plasticizer,<sup>12</sup> and so on. As a result, the Huisgen reaction has been attempted as the curing strategy of GAP binder via chemical linkage between azide groups in GAP and alkynyl compounds.<sup>13–19</sup> This kind of orthogonal ligation reaction is one of classical click reaction and gains considerable attention due to the fact that it is virtually quantitative, very robust and general.<sup>20</sup> Especially for preparing solid propellant, such reaction will not be interfered by other function groups and can generate high yields of target products without byproducts. Furthermore, compared with urethane curing strategy, a readily formation of triazole linkages eliminates the sensitivity of the whole curing system to surrounding humidity in both manufacture and storage process. On the other hand, the triazole linkages formed by Huisgen reaction can overcome the self-extinguishing in combustion under low pressure and enhance the burning rate of propellant.<sup>21,22</sup> As a result, bis-propargyl succinate (BPS) was used as a dipolarophile curing agent for GAP. Although the BPS-cured GAP materials showed a slightly higher glass-transition temperature than the GAP-based materials cured with hexamethylene diisocyanate trimer (abbreviation as N100),<sup>23</sup> the total adding amount of BPS to realize necessary crosslinking densities was less than that of N100, namely the loading-level of energetic GAP was relatively higher in the BPS-cured materials. In addition, the Huisgen reaction has also been used to improve the compatibility of the composites consisting of non-polar polybutadiene (PB) and polar GAP.<sup>24</sup> Hydroxyl-terminated PB was firstly reacted with propargyl bromide to produce propargyl-terminated polymer (PTPB), and then blended with GAP to form the triazole-crosslinked composites via 1,3-dipolar cycloaddition reaction under the catalysis of Cu(I)Cl at ambient temperature. The reaction between terminated-alkynyl groups of PTPB and azide groups of GAP directly realized the curing of two binders, and the crosslinking densities and mechanical properties of the as-prepared composites could be regulated by changing the molar ratio of azide group vs. alkynyl group. However, compared with those system cured by small molecules containing equivalent alkynyl groups, the loading-level of energetic GAP in the PTPB/GAP composites was relatively lower.

In this work, a diacetylene-functionalized compound, i.e., dimethyl 2,2-di(prop-2-ynyl)malonate (DDPM), were used as the

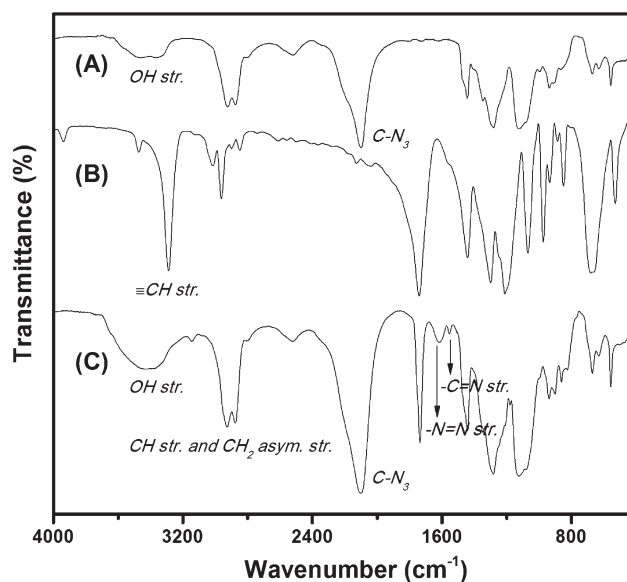


**Figure 1.** FTIR spectra of GAP (A), DDPM (B), and the DDPM/GAP film (C).

curing agent of GAP, and hence produced energetic materials with higher loading-level of GAP through Huisgen reaction. In our opinion, polar ester groups in DDPM might contribute to a good compatibility with highly polar GAP. By changing the feeding molar ratio of DDPM vs. GAP from 1 : 1 to 1 : 5, the molar ratio of alkynyl group vs. azide group in the whole system was regulated correspondingly, and hence affected the crosslinking densities of triazole-based network in the cured materials. Moreover, tensile test, swelling test, differential scanning calorimetry (DSC) analysis, dynamic mechanical analysis (DMA) and scanning electron microscopy (SEM) observation were carried out to investigate the structure–properties relationship of the DDPM-cured GAP materials.

## EXPERIMENTAL

### Materials

Dimethyl malonate and propargyl bromide (80 wt % in toluene, ca. 9.2 mol L<sup>-1</sup>) were purchased from J&K Scientific Ltd. (China). Sodium hydride (70 wt % dispersion in Mineral oil) and ammonium chloride were purchased from Wuhan Shenshi Chemical Technology Co. Ltd. (China). GAP with molecular weight of 3400 g mol<sup>-1</sup> and azide value of 9.995 mmol g<sup>-1</sup> was provided from the 42nd Institute of the Fourth Academy of China Aerospace Science and Technology Corporation (China). Cu(I)Cl (AR), tetrahydrofuran (THF, AR), acetic ether (EtOAc, AR), and *n*-Hexane as well as anhydrous magnesium sulfate were purchased from Sinopharm Chemical Reagent Co. Ltd. (China). THF was refluxed with a mixture of Na and benzophenone ketyl under nitrogen atmosphere and then distilled for usage.

### Synthesis of Dimethyl 2,2-di(prop-2-ynyl)malonate (DDPM)

First, sodium hydride (3.42g, 70 wt % dispersion in mineral oil) in 40 mL of THF was added into a 500-mL three-neck round bottom flask equipped with magnetic stirrer, thermometer and reflux condenser. A solution of dimethyl malonate (4.86

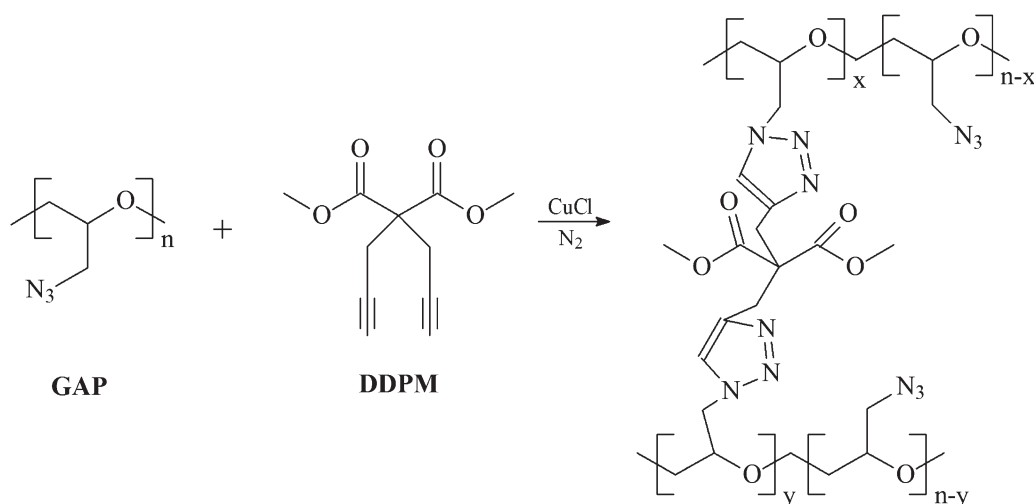


**Figure 2.** Schematic illustration of the reaction between DDPM and GAP.

mL) in 40 mL of THF was added dropwise at room temperature and reacted for an hour. Thereafter, a solution of propargyl bromide (10.2 mL, 80 wt % in toluene, ca.  $9.2 \text{ mol}\cdot\text{L}^{-1}$ ) in 100 mL of THF were added dropwise into the above mixture. Meanwhile, the reactant was allowed to reflux under  $110^\circ\text{C}$  for another 3 hours, and then cooled down to room temperature. Subsequently, the reaction products were extracted with 100 mL of saturated ammonium chloride by three times to get the organic layer, and the aqueous layer was extracted with 100 mL of diethyl ether by three times to get the residual organic substances. The organic layer together with the organic substances derived from the aqueous layer was dried over anhydrous  $\text{MgSO}_4$ , followed by removing the solvent via evaporation to obtain a light yellow solid. Finally, this crude product was purified by re-crystallization with the eluent of *n*-Hexane/EtOAc (6 : 1 by volume) to give the white solid product (yield 76.4%). Figure 1(B) show the Fourier transform infrared (FTIR) spectrum of DDPM. In the Figure 1(B), the predominant peak located at  $3292 \text{ cm}^{-1}$ , which was assigned to propargyl group, was observed. Moreover, the  $^1\text{H-NMR}$  spectrum of DDPM distinctly presented three peaks located at 2.05 ppm (*t*,  $J = 2.7 \text{ Hz}$ , 2H), 3.01 ppm (*d*,  $J = 2.7 \text{ Hz}$ , 4H) and 3.77 ppm (*s*, 6H), which were assigned to proton resonance in  $-\text{CH}$ ,  $-\text{CH}_2$ , and  $-\text{CH}_3$  in the DDPM.<sup>25</sup> The results mentioned above verified the structure and purity of the alkylated dimethyl malonate.

#### Preparation of the DDPM/GAP Films via 1,3-Dipolar Cycloaddition

According to the specified molar ratio of DDPM vs. GAP as 1 : 1, 2 : 1, 3 : 1, 4 : 1, and 5 : 1, a given amount of DDPM in THF (100 mL) and the corresponding stoichiometric ratio of GAP in THF (200 mL) were mixed into a 500-mL three-neck round bottom flask while a catalyzer of  $\text{Cu(I)Cl}$  was added into the reactant solution. Subsequently, the reaction was mechanically stirred under nitrogen atmosphere at the ambient temperature for 12 h in the dark. Figure 2 depicts the reaction between DDPM and GAP under the catalysis of  $\text{Cu(I)Cl}$ . After the reaction, the  $\text{Cu(I)Cl}$  was removed by filtration and the reaction solution was condensed by rotating evaporation. Finally, the

condensed reaction solution was casted into a Teflon mold, and conditioned for 3 days at ambient temperature to obtain the solidified film. All the films were vacuum-dried for 4 hours before dry preservation, and coded as DDPM/GAP-1, DDPM/GAP-2, DDPM/GAP-3, DDPM/GAP-4, and DDPM/GAP-5, respectively. Herein, the arabic numerals represented the feeding molar ratio values of DDPM vs. GAP.

#### Characterization

FTIR spectroscopy measurement of the DDPM, GAP and the DDPM/GAP film was carried out on an FTIR 5700 spectrometer (Nicolet, Madison, WI) in the range of  $4000\text{--}400 \text{ cm}^{-1}$ .  $^1\text{H}$  NMR spectra of DDPM was recorded on a Bruker 500 MHz spectrometer at ambient temperature. Tetramethylsilane (TMS) was used as internal standard and  $\text{CDCl}_3$  was used as solvent.

DSC analysis was performed on a Q20 DSC (TA instruments, DE) under a nitrogen atmosphere in the range of  $-150$  to  $100^\circ\text{C}$  with a heating rate of  $20^\circ\text{C min}^{-1}$ . Before the test, the specimens were heated from room temperature to  $100^\circ\text{C}$  and then cooled down to  $-150^\circ\text{C}$  with a cooling rate of  $20^\circ\text{C min}^{-1}$  to eliminate thermal history. Dynamic mechanical tests were carried out by means of a DMA 242C (Netzsch, Hanau, Germany) with a dual cantilever device at a frequency of 1 Hz. The temperature range was from  $-80$  to  $160^\circ\text{C}$  with a heating rate of  $3^\circ\text{C min}^{-1}$ . The size of testing specimens was  $30 \text{ mm} \times 10 \text{ mm}$ .

SEM observation was carried out on a VEGA 3 LMU scanning electron microscope (TESCAN, Czech Republic). All the DDPM-crosslinked GAP films were frozen in liquid nitrogen and then snapped immediately. The fracture surfaces of the fractured films were sputtered with gold and then photographed.

Mechanical properties, including the parameters of tensile strength ( $\sigma_b$ ), elongation at break ( $\epsilon_b$ ), and Young's modulus ( $E$ ), of all the DDPM/GAP films were measured on a CMT6503 universal testing machine (SANS, Shenzhen, China) with a tensile rate of  $50 \text{ mm min}^{-1}$ . The testing films were cut into strips with a width of 10 mm and a distance between testing marks was 30 mm. The testing strips were kept at 0% humidity for

7 days before measurement. A mean value of five replicates from each film was taken.

Crosslinking density ( $\gamma$ ) can be defined as the number of moles in the effective network chain per cubic centimeter, and is generally obtained from the volume fraction of the swollen polymer in a solvent ( $\varphi$ ) and the gel fraction of the swollen polymer ( $\omega$ ) according to the following eq. (1). Moreover, the parameters of  $\varphi$  and  $\omega$  can be calculated as the following eqs. (2) and (3),<sup>26</sup> respectively.

$$\gamma = \phi^{5/3} \cdot \omega \quad (1)$$

$$\varphi = \frac{m_0/\rho_2}{m/\rho_1 + m_0(1/\rho_2 - 1/\rho_1)} \quad (2)$$

$$\omega = \frac{m_1}{m} \times 100\% \quad (3)$$

where  $\rho_1$  and  $\rho_2$  are respectively the densities of solvent (0.87 g cm<sup>-3</sup> for toluene in this work) and the testing specimens (The densities of the DDPM/GAP films with the feeding molar ratios of DDPM vs. GAP were taken as a mean value of 1.27 g cm<sup>-3</sup>) while  $m_0$ ,  $m$ , and  $m_1$  represent the weights of the initial, swollen, and deswollen states, respectively. For the measurement of crosslinking density, the whole experiment process is depicted as follows: Before the testing, the soluble substances in the testing specimen were firstly extracted by acetone for four days, and then the specimen was dried and its density ( $\rho$ ) was measured by the method of specific gravity bottle. Subsequently, the testing specimens of the DDPM/GAP films were placed in toluene for 7 days for swelling. Finally, the swollen specimens were weighed after removing the solvent attached on the specimen surface with filter paper. Furthermore, the absorbed solvent of swollen specimens evaporated for re-weighing the deswollen specimen.

## RESULTS AND DISCUSSION

### Structure of the DDPM-Crosslinked GAP Materials

As shown in Figure 2, two alkynyl groups of DDPM can react with the arbitrary azide group in GAP, and hence bridge two GAP chains to form crosslinked structure. Moreover, the predominant character of the reaction product is the formation of triazole structure. As a result, the FTIR was used to trace the structural changes after the reaction between DDPM and GAP. Figure 1 shows the FTIR spectra of GAP (A) DDPM (B) and the DDPM/GAP film (C). In this work, even though the feeding molar ratio of DDPM vs. GAP reached 5 : 1, the azide groups in the whole system were still excessive. As a result, the peak located at 3292 cm<sup>-1</sup> in Figure 1(B), which was assigned to -CH stretching vibration of the alkynyl group in DDPM, disappeared in Figure 1(C) of the DDPM/GAP film. However, excessive azide groups presented a peak located at 2101 cm<sup>-1</sup>, and the peak shape and location were in agreement with those of neat GAP in Figure 1(A). On the other hand, three emerging absorptions were observed at 3145, 1620, and 1555 cm<sup>-1</sup> in Figure 1(C), which were assigned to -CH stretching vibration, -N=N skeletal vibration and -C=N skeletal vibration of the formed triazole ring, respectively. Overall, the appearance of such three absorptions assigned to the triazole ring, together

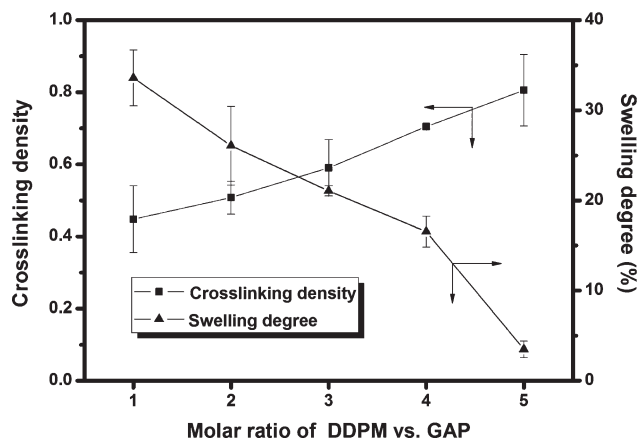


**Figure 3.** Effect of the molar ratio of DDPM vs. GAP on the swelling degree and crosslinking densities of the DDPM/GAP films.

with the absence of -CH stretching vibration of alkynyl group, in Figure 1(C) verified the occurrence of reaction between DDPM and GAP, which provided the triazole linkage to the formation of network in the solidified DDPM/GAP film.

### Swelling Behaviors and Crosslinking Densities of the DDPM-Crosslinked GAP Materials

For network-structured materials, the crosslinking density is a dominant factor to determining mechanical performances. In this work, by changing the feeding molar ratio of DDPM vs. GAP, the crosslinking densities were regulated due to different stoichiometric ratio of alkynyl and azide groups. Figure 3 shows the effects of the molar ratios of DDPM vs. GAP on the crosslinking densities ( $\gamma$ ) and swelling degrees of the as-prepared DDPM/GAP films. The increase of crosslinking points can inhibit the swelling behavior. As usual, the dependence of crosslinking density upon the molar ratios of DDPM vs. GAP was opposite to that of swelling degree. With an increase in the feeding molar ratio of DDPM vs. GAP from 1 : 1 to 5 : 1, more alkynyl groups were supplemented to react with the azide groups in the GAP chains, and hence formed more triazole linkages as crosslinking points. As a result, the crosslinking densities increased from 0.45 to the maximum value of 0.81 with an increase in the feeding molar ratio of DDPM vs. GAP while the swelling degrees decreased from 33.6% to the minimum value of 3.5%.

### Mechanical Properties of the DDPM-Crosslinked GAP Materials

Figure 4 shows the effects of the molar ratios of DDPM vs. GAP on tensile strength ( $\sigma_b$ ), breaking elongation ( $\epsilon_b$ ), and Young's modulus ( $E$ ) of the DDPM/GAP films. With an increase in the molar ratios of DDPM vs. GAP, the Young's modulus and tensile strength of the DDPM/GAP films gradually increased. However, the whole tendency could be divided two stages. First, when the molar ratio of DDPM vs. GAP was lower than 3 : 1, the increment of Young's modulus and tensile strength were relatively small. However, when the molar ratio of DDPM vs. GAP was higher than 4 : 1, there were significant increase for the Young's modulus and tensile strength by ca. 1500% and ca.280%, respectively, in contrast to the DDPM/



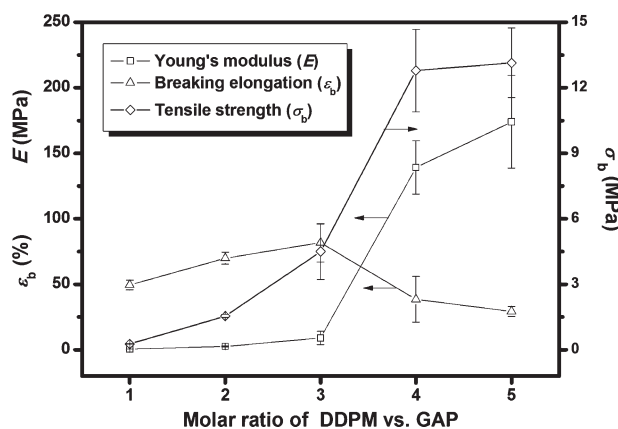


**Figure 4.** Effect of the molar ratio of DDPM vs. GAP on the tensile strength ( $\sigma_b$ ), breaking elongation ( $\varepsilon_b$ ), and Young's modulus ( $E$ ) for the DDPM/GAP films.

GAP film with a molar ratio of 3 : 1. The DDPM/GAP film with a molar ratio of 5 : 1 showed the maximum values of 174.1 MPa in Young's modulus and 13.1 MPa in tensile strength. In theory, the change of breaking elongation is usually opposite to that of Young's modulus. However, in this work, the breaking elongation of DDPM/GAP films firstly increased with an increase in the molar ratio of DDPM vs. GAP up to 3 : 1, and then decreased. The DDPM/GAP film with a molar ratio of 3 : 1 showed the maximum value of 81.7%. It was worth of noting that the maximum values of Young's modulus and tensile strength for the DDPM/GAP materials were obviously higher than those reported values of the GAP-based materials cured with other alkynyl compounds of BPS<sup>23</sup> and PTPB.<sup>24</sup> Furthermore, when the values of breaking elongation for three kinds of GAP-based materials cured with DDPM, BPS and PTPB were equivalent with each other (above 80%), the DDPM/GAP material still showed the highest Young's modulus and tensile strength.

As well-known, higher crosslinking densities can contribute to the enhancement of Young's modulus and tensile strength, and results in the decrease of breaking elongation. In this work, with an increase of crosslinking densities, the Young's modulus and tensile strength of the DDPM/GAP films normally increased. However, the breaking elongation showed a tendency of increasing firstly and subsequently decreasing, and the highest breaking elongation happened at the molar ratio of DDPM vs. GAP as 3 : 1. The lower breaking elongation of the DDPM/GAP films with the molar ratio lower than 2 : 1 might be ascribed to the relatively poor tensile strength and Young's modulus. The films snapped before the chains could not fully stretch in the tensile process. Fundamentally, no enough triazole linkage might result in the failure of the formation of tough network. When the molar ratio of DDPM vs. GAP was higher than 3.0, more alkynyl groups participated into forming the triazole-based network. At this time, the increase of crosslinking points inhibited the deformation of the resultant films and ensured adequate stress transferring balance. Consequently, the Young's modulus and tensile strength increased with an expense of breaking elongation.

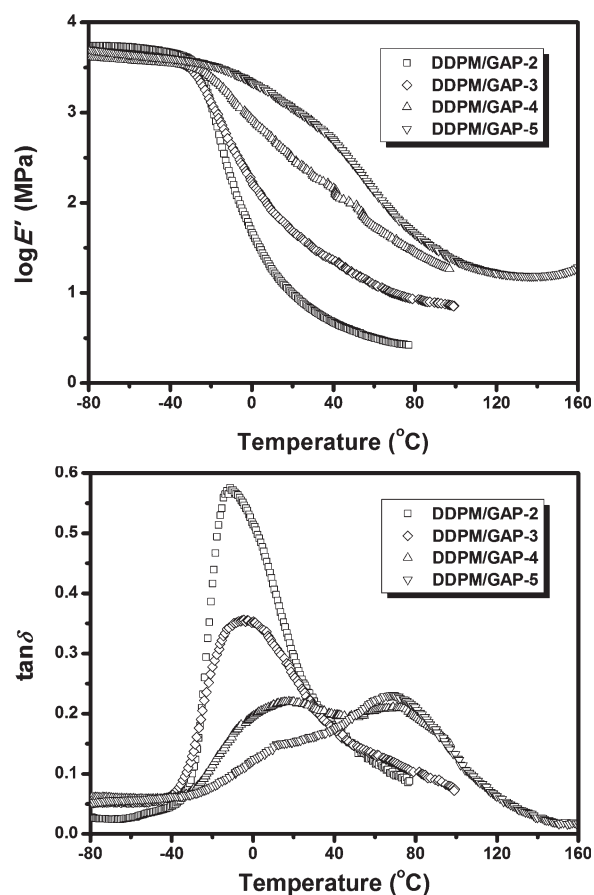


**Figure 5.** Dependence of storage modulus ( $\log E'$ ) and loss factor ( $\tan \delta$ ) upon temperature for the DDPM/GAP films with various feeding molar ratios of DDPM vs. GAP.

#### Thermal Properties of the DDPM-Crosslinked GAP Materials

Table I summarized the glass transition temperature ( $T_g$ ) and the increment of heat capacity ( $\Delta C_p$ ) of the DDPM/GAP films measured by DSC. With the increase in the molar ratio of DDPM vs. GAP, the  $T_g$  values of the DDPM/GAP films gradually increased from  $-43.9^\circ\text{C}$  to  $-5.1^\circ\text{C}$ . With an increase of crosslinking densities, the network structure became denser together with the shortening of the distance among crosslinking points. As a result, the shift of  $T_g$  up to high temperature was ascribed to the fact that the increase of crosslinking densities aggravated the inhibition to the motion of the segments in GAP. Compared with the revealing of domain-scale segmental motion by the specific heat increment of glass transition from the DSC test, DMA is a powerful technique to investigate the molecular-level motion of glassy segments through  $\alpha$ -relaxation. Figure 5 depicts dependence of storage modulus ( $\log E'$ ) and loss factor ( $\tan \delta$ ) upon temperature for the cured DDPM/GAP films with various feeding molar ratios of DDPM vs. GAP, and the results of  $\alpha$ -relaxation temperature ( $T_\alpha$ ) and loss factor ( $\tan \delta$ ) for each loss peak were summarized in Table I. Due to a crack in the heating process, the curves and related data of the DDPM/GAP-1 film failed to determine. Similar to the DSC results, the  $T_\alpha$  values of the DDPM/GAP films also significantly increased with an increase in the molar ratio of DDPM vs.

**Table I.** SC and DMA Data of the DDPM/GAP Films with Various Feeding Molar Ratios of DDPM vs. GAP

Sample No.	DSC data		DMA data			
	$T_g$ (°C)	$\Delta C_p$ (J g <sup>-1</sup> ·K <sup>-1</sup> )	$T_{x1,max}$ (°C)	tan $\delta$	$T_{x2,max}$ (°C)	tan $\delta$
DDPM/GAP-1	-43.9	0.45	n.d.	n.d.	n.d.	n.d.
DDPM/GAP-2	-39.7	0.39	-12.9	0.57	—	—
DDPM/GAP-3	-34.1	0.22	-4.6	0.38	—	—
DDPM/GAP-4	-9.7	0.36	12.5	0.22	67.1	0.21
DDPM/GAP-5	-5.1	0.15	14.9	0.15	71.2	0.23

GAP. At the same time, the drop zone of storage modulus also shifted up to high temperature. However, when the molar ratio of DDPM vs. GAP was higher than 4 : 1, two loss peaks were observed in the tan  $\delta$ - $T$  curves. It indicated that more crosslinking points led to the obvious structural heterogeneity in the DDPM/GAP films. The loss peak located at high temperature might be assigned to the segments close to crosslinking points.

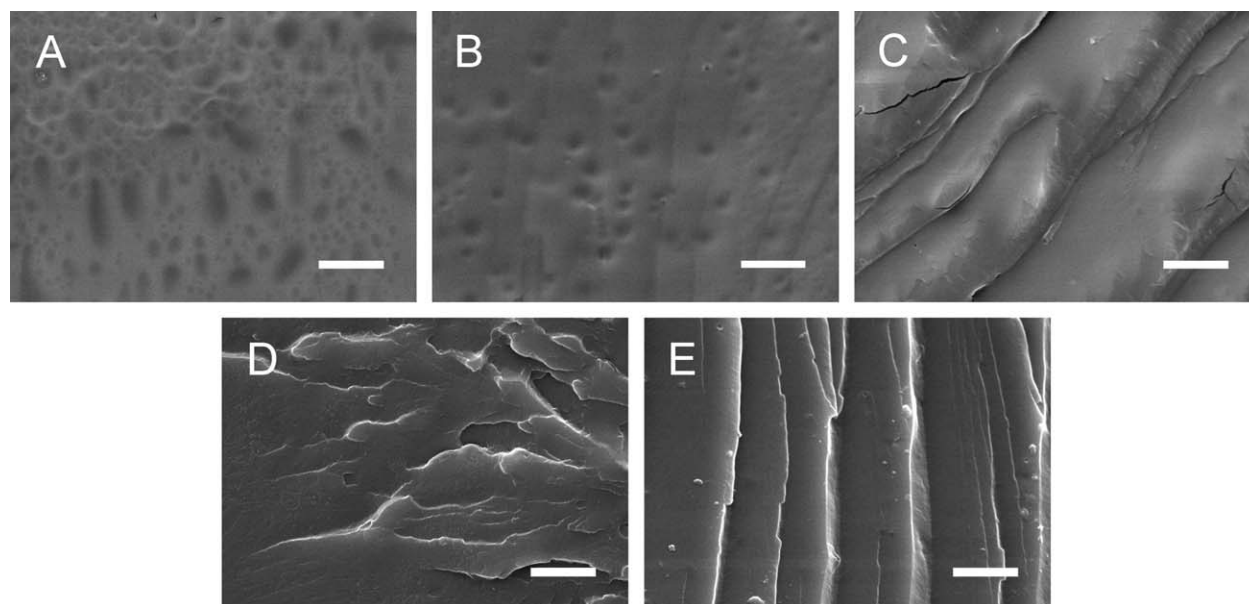
#### Fractured Morphologies of the DDPM-Crosslinked GAP Materials

Figure 6 depicts the morphologies of the fractured surfaces of the DDPM/GAP films with various molar ratios of DDPM vs. GAP. With an increase in the molar ratio of DDPM vs. GAP, the wrinkle and ravines of the fractured surfaces were more and more obvious while the fractured stripes became deeper. It might be ascribed to the fact that the structural heterogeneity in the DDPM/GAP films gradually aggravated with an increase of crosslinking densities.

#### CONCLUSIONS

In this work, an alkynyl compound, i.e., DDPM, was synthesized via the reaction between propargyl bromide and dimethyl

malonate, and hence used as the curing agent for GAP. By regulating the feeding molar ratio of DDPM vs. GAP, a series of triazole-crosslinked materials with various crosslinking densities were prepared via 1,3-dipolar cycloaddition reaction between alkynyl and azide groups. The tensile strength and Young's modulus of the as-prepared DDPM/GAP films increased with an increase of the crosslinking densities. The maximum tensile strength and Young's modulus were 13.1 MPa and 174.1 MPa, respectively, for the DDPM/GAP film with a molar ratio of 5 : 1. At the same time, the DDPM/GAP film with a molar ratio of 3 : 1 showed the highest breaking elongation of 81.7% together with 4.5 MPa in tensile strength and 9.1 MPa in Young's modulus. The increase of crosslinking densities resulted in the shift of glass transition up to high temperature and the structural heterogeneity in the DDPM/GAP materials. The latter was shown as two loss peaks in the tan  $\delta$ - $T$  curves for the DDPM/GAP materials with the molar ratio higher than 4 : 1 and rougher fractured surface with an increase in the molar ratio of DDPM vs. GAP. On the whole, the DDPM shows a great potential as the curing agent of GAP binders, and the regulation of the crosslinking density is expected to optimize mechanical and thermal properties of the resultant energetic materials to meet the



**Figure 6.** SEM images for the fractured surfaces of the films coded as DDPM/GAP-1 (A), DDPM/GAP-2 (B), DDPM/GAP-3 (C), DDPM/GAP-4 (D), and DDPM/GAP-5 (E) (The scale in the images is 10  $\mu$ m.).

requirement of composite solid propellant. Furthermore, compared with urethane curing method, the curing mechanism based on Huisgen reaction contributes to the additional advantages of humidity-insensitivity and good compatibility with other high-energy ingredients in propellant.

#### ACKNOWLEDGMENTS

This work was supported by the Program of New Century Excellent Talents, Ministry of Education of China (NCET-11-0686); Fundamental Research Funds for the Central Universities (Self-Determined and Innovative Research Funds of WUT 2012-Ia-006).

#### REFERENCES

1. Gaur, B.; Bimlesh, L.; Choudhary, V.; Varma, I. K. *J. Macromol. Sci. Part C-Polym. Rev.* **2003**, *43*, 505.
2. Frankel, M. B.; Grant, L. R.; Flanagan, J. E. *J. Propulsion Power* **1992**, *8*, 560.
3. Ross, G. S.; Mark Husband, D. *Propell. Explos. Pyrotech.* **1991**, *16*, 167.
4. Selim, K.; Özkaz, S.; Yilmaz, L. *J. Appl. Polym. Sci.* **2000**, *77*, 538.
5. Min, B. S.; Park, Y. C.; Yoo, J. C. *Propell. Explos. Pyrotech.* **2012**, *37*, 59.
6. Hocaoglu, O.; Ozbelge, T.; Pekel, F.; Ozkar, S. *J. Appl. Polym. Sci.* **2002**, *84*, 2072.
7. Manjari, R.; Somasundaram, U. I.; Joseph, V. C.; Sriram, T. *J. Appl. Polym. Sci.* **1993**, *48*, 279.
8. Min, B. S.; Baek, G.; Ko, S. W. *J. Ind. Eng. Chem.* **2007**, *13*, 373.
9. Mathew, S.; Manu, S. K.; Varghese, T. L. *Propell. Explos. Pyrotech.* **2008**, *33*, 146.
10. Manu, S. K.; Varghese, T. L.; Mathew, S.; Ninan, K. N. *J. Appl. Polym. Sci.* **2009**, *114*, 3360.
11. Manu, S. K.; Sekkar, V.; Scariah, K. J.; Varghese, T. L.; Mathew, S. *J. Appl. Polym. Sci.* **2008**, *110*, 908.
12. Reed R. Jr. U.S. Pat. 6,103,029, 2000.
13. Lutz J. F. *Angew. Chem. Int. Ed.* **2007**, *46*, 1018.
14. Van Steenis, D. J. V. C.; David, O. R. P.; Van Strijdonck, G. P. F.; Van Maarseveen, J. H.; Reek, J. N. H. *Chem. Commun.* **2005**, *34*, 4333.
15. Gunay, U. S.; Durmaz, H.; Gungor, E.; Dag, A.; Hizal, G.; Tunca, U. *J. Appl. Polym. Sci. Part A: Polym. Chem.* **2012**, *50*, 729.
16. Binder, W. H.; Sachsenhofer, R. *Macromol. Rapid Commun.* **2007**, *28*, 15.
17. Su, H.; Zheng, J. K.; Wang, Z.; Lin, F.; Feng, X. Y.; Dong, X. H.; Becker, M. L.; Cheng, S. Z. D.; Zhang, W. B.; Li, Y. W. *ACS Macro Lett.* **2013**, *2*, 645.
18. Wang, Z.; Li, Y. H.; Dong, X. H.; Yu, X. F.; Guo, K.; Su, H.; Yue, K.; Wesdemiotis, C.; Cheng, S. Z. D.; Zhang, W. B. *Chem. Sci.* **2013**, *4*, 1345.
19. Golasa, P. L.; Matyjaszewski, K. *Chem. Soc. Rev.* **2010**, *39*, 1338.
20. Rostovtsev, V. V.; Green, L. G.; Fokin, V. V.; Sharpless, K. B. *Angew. Chem. Int. Ed.* **2002**, *41*, 2596.
21. Dubois, C.; Dësilets, S.; Nadeau, G.; Gagnon, N. *Propell. Explos. Pyrotech.* **2003**, *28*, 107.
22. Manzara, A. P. U.S. Pat. 5,681,904, 1997.
23. Keicher, T.; Kuglstatte, W.; Eisele, S.; Wetzel, T.; Krause, H. *Propell. Explos. Pyrotech.* **2009**, *34*, 210.
24. Ding, Y.; Hu, C.; Guo, X.; Che, Y.; Huang, J. *J. Appl. Polym. Sci.*, **2014**, DOI: 10.1002/app.40007.
25. Severa, K.; Vávra, J.; Kohoutová, A.; Čížková, M.; Šálová, T.; Hývl, J.; Šaman, D.; Pohl, R.; Adriaenssens, L.; Teplý, F. *Tetrahedron Lett.* **2009**, *50*, 4526.
26. Lu, M.; Huang, Z. P.; Song, Y. L. *J. Solid Rocket Technol.* **1994**, *3*, 54.